J. Plasma Physics (2000), *vol.* 64, *part* 5, *pp.* 613–621. Printed in the United Kingdom

Effect of pump depletion and self-focusing (hot spot) on stimulated Raman scattering in laser–plasma interaction

SALEH T. MAHMOUD and R. P. SHARMA
Centre for Energy Studies, IIT Delhi, New Delhi-110016, India

(Received 12 May 2000 and in revised form 13 June 2000)

Abstract. A three-dimensional study of the pump depletion and self-focusing (hot spot) effect on stimulated Raman scattering (SRS) reflectivity is presented within the paraxial-ray approximation. The reflectivity of SRS is observed to exhibit a maximum value in the case of optimum SRS gain with pump depletion. The reflectivity with pump depletion is less than without pump depletion and is the usual three-wave interaction case. The effect of plasma temperature on SRS reflectivity is also discussed.

1. Introduction

The reflection of laser light arising from parametric instabilities can be an important process in laser fusion plasmas. In particular, the Raman backscattering of laser light in an underdense region can prevent the light from arriving at the critical density where enhanced absorption occurs. Stimulated Raman scattering (SRS) is a major instability, which plays a very important role in laser–plasma interaction. The SRS instability is the resonant decay of the incident laser wave into a scattered electromagnetic (EM) wave and an electron plasma wave. This electron plasma wave can have a very high phase velocity (of the order of the velocity of light), and so can produce very energetic electrons when it damps (Kruer 1988). Such electrons can preheat the fuel in laser fusion applications. The Raman instability is of particularly significant concern because of large reflectivity and high-energy electrons. Control of laser–plasma instabilities such as SRS is very important for the success of laser fusion. Much experimental and theoretical work has been devoted to the study of the SRS instability (Thomson 1978; Karttunen 1980; Antonsen and More 1992; Kolber et al. 1993; Fernandez et al. 1996; Divol and Mounaix 1998; Tzeng and Mori 1999; Berger et al. 1999; Baker et al. 1999). In spite of the great deal of interest in SRS, the nonlinear saturation of the Raman process is not yet fully understood.

Different mechanisms have been proposed to explain the nonlinear saturation of the SRS process. One of these mechanisms involves competition between SRS and stimulated Brillouin scattering (SBS). Walsh et al. (1984) observed a strong correlation between the quenching of an SRS plasma wave and the initiation of an SBS ion wave. Another possible nonlinear mechanism may arise from further parametric decay of the SRS Langmuir wave (LW) into an ion acoustic wave (IAW) and another LW, as has been seen experimentally by Baker et al. (1996). Self-focusing instability may also be one of the mechanisms

that may affect the SRS process. When a laser beam of finite size, having non-uniform intensity distribution along its wave front, propagates in a plasma, it modifies the background plasma density distribution and undergoes strong self-focusing (hot spot). Thus the scattering of a laser beam should be strongly affected by the non-uniformity in the intensity distribution of the laser. Recently, Russell et al. (1999) used a two-dimensional simulation to study nonlinear SRS from a laser hot spot when the LW from SRS processes further decays into another LW and an IAW. They have studied the effect of self-focusing on SRS reflectivity, and have shown that in the case of self-focusing, the density profile has a V shape with a strong density gradient in the direction of beam propagation (denoted by y). Without self-focusing, there is a density channel resulting from the ponderomotive pressure of LWs, but it has a relatively flat profile along y. These results predict that the ponderomotive modification of the density profile appears to significantly lower the reflectivity by a factor of three. Russell et al. (1999) also found that density-profile modification and, in the case of higher laser intensity, pump depletion reduced the reflectivity at $T_e = 1$ keV. Pump depletion and ponderomotive density-profile modification can reduce the dependence of the reflectivity on the IAW damping-to-frequency ratio.

The motivation of the present work is to study nonlinear SRS in three-dimensional geometry within the paraxial-ray approximation. The main emphasis here is on the effect of pump depletion on self-focusing of the pump laser beam, the stimulated backscattered laser beam, and consequently on the SRS back-reflectivity. It has been demonstrated that the self-focusing effect modifies the Raman gain through modified intensity and modified density due to hot spots, and consequently the SRS reflectivity is affected. These two effects (intensity/density) have the opposite effect on SRS gain, and the optimum value of the intensity of laser power has been predicted when the gain is maximum.

This paper is organized as follows. Section 2 describes the theoretical model of SRS reflectivity in the presence of steady-state pump self-focusing and pump depletion. Section 3 summarizes the main results from three-dimensional simulation and the effect of various parameters that affect this reflectivity.

2. Model equation

A Gaussian laser beam is considered to be propagating in a hot, collisionless, and homogenous plasma along the z direction; the initial intensity distribution of the beam is given by

$$E_0 E_0^* |_{z=0} = E_{00}^2 \exp\left(-\frac{r^2}{r_0^2}\right), \tag{1}$$

where r is the radial coordinate of the cylindrical coordinate system and E_{00} is the axial amplitude. The laser beam f-number F is defined as the ratio of the beam waist r_0 to the laser vacuum wavelength ($\lambda_0 = 2\pi c/\omega_0$). To study the scattering of the laser beam from an electrostatic wave in the plasma, we use the wave equation

$$\nabla^2 \mathbf{E} - \nabla(\mathbf{E}\cdot\nabla \ln \epsilon) = \frac{1}{c^2}\frac{\partial^2 \mathbf{E}}{\partial t^2} + \frac{4\pi}{c^2}\frac{\partial \mathbf{J}}{\partial t} \tag{2}$$

https://doi.org/10.1017/S0022377800008898 Published online by Cambridge University Press

where ϵ is the dielectric constant of the plasma and $\mathbf{J}$ is the total current density in the presence of the wave. The total electric field $\mathbf{E}$ in the plasma may be expressed as

$$\mathbf{E} = \mathbf{E}_0 \exp(\omega_0 t) + \mathbf{E}_s \exp(\omega_s t), \tag{3}$$

where $\mathbf{E}_0$ is the electric vector of the pump beam and $\mathbf{E}_s$ is the electric vector of the scattered wave. In this three-wave interaction (pump wave, plasma wave, and scattered wave), the phase-matching condition is given by

$$\omega_0 = \omega_s + \omega, \qquad k_0 = k_s + k,$$

where ω_0 (ω_s) and k_0 (k_s) are the angular frequency and wavenumber of the incident (scattered) wave respectively, and ω and k are the frequency and wavenumber of the electron plasma wave. From (2) and (3), one obtains the following equations governing the pump and scattered laser beam:

$$\nabla^2 E_0 + \frac{\omega_0^2}{c^2}\left(1 - \frac{\omega_{pe}^2}{\omega_0^2}\frac{N_0}{N_{00}}\right)E_0 = -\frac{4\pi e}{c^2}\frac{1}{2}\frac{\partial}{\partial t}(N_e V_0), \tag{4}$$

$$\nabla^2 E_s + \frac{\omega_s^2}{c^2}\left(1 - \frac{\omega_{pe}^2}{\omega_s^2}\frac{N_0}{N_{00}}\right)E_s = -\frac{4\pi e}{c^2}\frac{1}{2}\frac{\partial}{\partial t}(N_e^* V_s). \tag{5}$$

Here N_0 is the background density, modified on account of the transverse intensity gradients of the pump and scattered beam, and ω_{pe} is the plasma frequency. The transverse intensity gradient generates a ponderomotive force, which modifies the plasma density profile in the transverse direction. This is given by

$$N_0 = N_{00} \exp\left(-\frac{3}{4}\alpha_0 \frac{m}{M} E_0 E_0^* - \frac{3}{4}\alpha_s \frac{m}{M} E_s E_s^*\right), \tag{6}$$

where

$$\alpha_{0,s} = \frac{e^2 M}{6 k_B T_e \gamma_e m^2 \omega_{0,s}^2},$$

N_{00} is the background electron density of the plasma in the absence of the laser beam, e and m are the electron charge and mass respectively, M is the ion mass, k_B is Boltzmann's constant, γ_e is the ratio of specific heats for the electron gas, and is taken equal to 3, and T_e is the equilibrium plasma temperature. In (4) and (5), N_e is the electron density perturbation in the electron plasma wave. Following the standard technique, one obtains the following equations for the pump and scattered beam respectively (Kruer 1988):

$$\nabla^2 E_0 + \frac{\omega_0^2}{c^2}\left(1 - \frac{\omega_{pe}^2}{\omega_0^2}\frac{N_0}{N_{00}}\right)E_0 = \frac{N_0}{N_{00}}\omega_{pe}^2 \frac{e^2 k^2 |E_s E_s^*| E_s}{8 m_e^2 \omega_0 \omega_s^2 c^2 2i\Gamma_e}, \tag{7}$$

$$\nabla^2 E_s + \frac{\omega_s^2}{c^2}\left(1 - \frac{\omega_{pe}^2}{\omega_s^2}\frac{N_0}{N_{00}}\right)E_s = \frac{N_0}{N_{00}}\omega_{pe}^2 \frac{e^2 k^2 |E_0 E_0^*| E_s}{8 m_e^2 \omega_0^2 \omega_s c^2 2i\Gamma_e}. \tag{8}$$

Using the paraxial-ray approximation, one can solve these coupled equations (7) and (8). Writing

$$E_0 = A_{00}(x,y,z) \exp\left(i\{\omega_0 t - k_0[z + s_0(x,y,z)]\}\right),$$
$$E_s = A_{s0}(x,y,z) \exp\left(i\{\omega_s t - k_s[z + s_s(x,y,z)]\}\right),$$

https://doi.org/10.1017/S0022377800008898 Published online by Cambridge University Press

substituting these into (7) and (8), respectively, and separating the real and imaginary parts, the following sets of coupled equations are obtained. Equation (7) gives

$$\frac{\partial A_{00}^2}{\partial z}+\frac{\partial A_{00}^2}{\partial x}\frac{\partial s_0}{\partial x}+\frac{\partial A_{00}^2}{\partial y}\frac{\partial s_0}{\partial y}+\left(\frac{\partial^2 s_0}{\partial x^2}+\frac{\partial^2 s_0}{\partial y^2}\right)A_{00}^2+\frac{N_0}{N_{00}}\frac{e^2\omega_{pe}^2 k^2|A_s|^2}{8m_e^2\omega_0^2\omega_s^2 2\Gamma_e c\epsilon^{1/2}}A_{00}^2=0, \tag{9}$$

$$2\frac{\partial s_0}{\partial z}+\left(\frac{\partial s_0}{\partial x}\right)^2+\left(\frac{\partial s_0}{\partial y}\right)^2=-\frac{\omega_{pe}^2}{\omega_0^2}\left(\frac{N_0-N_{00}}{N_{00}\epsilon_0}\right)+\frac{1}{k_0^2 A_{00}}\left(\frac{\partial^2 A_{00}}{\partial x^2}+\frac{\partial^2 A_{00}}{\partial y^2}\right) \tag{10}$$

Similarly, (8) yields

$$\frac{\partial A_{s0}^2}{\partial z}+\frac{\partial A_{s0}^2}{\partial x}\frac{\partial s_s}{\partial x}+\frac{\partial A_{s0}^2}{\partial y}\frac{\partial s_s}{\partial y}+\left(\frac{\partial^2 s_s}{\partial x^2}+\frac{\partial^2 s_s}{\partial y^2}\right)A_{s0}^2-\frac{N_0}{N_{00}}\frac{e^2\omega_{pe}^2 k^2|A_0|^2}{8m_e^2\omega_0^2\omega_s^2 2\Gamma_e c\epsilon_s^{1/2}}A_{s0}^2=0, \tag{11}$$

$$2\frac{\partial s_s}{\partial z}+\left(\frac{\partial s_s}{\partial x}\right)^2+\left(\frac{\partial s_s}{\partial y}\right)^2=-\frac{\omega_{pe}^2}{\omega_s^2}\left(\frac{N_0-N_{00}}{N_{00}\epsilon_s}\right)+\frac{1}{k_s^2 A_{s0}}\left(\frac{\partial^2 A_{s0}}{\partial x^2}+\frac{\partial^2 A_{s0}}{\partial y^2}\right). \tag{12}$$

The solution of (9) and (10) can be written as (Akhmanov et al. 1968)

$$A_{00}^2=\frac{E_{00}^2(z=0)}{f_0^2(z)}\exp\left[-\frac{r^2}{r_0^2 f_0^2(z)}-2g_0 z\right], \tag{12a}$$

$$S_0=\frac{r^2}{2}\frac{1}{f_z(z)}\frac{df_0(z)}{dz}+\phi_0(z), \tag{12b}$$

$$g_0=\frac{e^2\omega_{pe}^2 k^2|A_s|_{r=0}^2(N_0/N_{00})_{r=0}}{16\,m_e^2\omega_0^2\omega_s^2\,\Gamma_e c\epsilon_0^{1/2}}. \tag{12c}$$

Similarly, for the scattered beam, we can get the following equations:

$$A_{s0}^2=\frac{E_{s0}^2(z'=0)}{f_s^2(z')}\exp\left[-\frac{r^2}{r_s^2 f_s^2(z')}-2g_s z'\right], \tag{13a}$$

$$S_s=\frac{r^2}{2}\frac{1}{f_s(z')}\frac{df_s(z')}{dz}+\phi_s(z'), \tag{13b}$$

$$g_s=\frac{-e^2\omega_{pe}^2 k^2|A_0|_{r=0}^2(N_0/N_{00})_{r=0}}{16\,m_e^2\omega_0^2\omega_s^2\,\Gamma_e c\epsilon^{1/2}}, \tag{13c}$$

$$g_s=-G_{srs}|A_0|_{r=0}^2\left(\frac{N_0}{N_{00}}\right)_{r=0}, \tag{13d}$$

where

$$G_{srs}=\frac{e^2\omega_{pe}^2 k^2 E_{00}^2}{16\,m_e^2\omega_0^2\omega_s^2\,\Gamma_e c\epsilon^{1/2}}. \tag{13e}$$

Here G_{srs} is the usual SRS gain for the three-wave interaction case, g_0 and g_s are the gain factors of the pump and scattered waves respectively, $z'=L_z-z$, L_z is the interaction length (which is approximately 250 times the free-space wavelength of the laser), and r_s is the beam width of the seed SRS at $z'=0$. In (12) and (13), f_0 and f_s are dimensionless beamwidth parameters for the pump

https://doi.org/10.1017/S0022377800008898 Published online by Cambridge University Press

and backscattered laser beams respectively. The differential equations governing f_0 and f_s are

$$\frac{d^2 f_0}{dz^2} = \frac{1}{k_0^2 r_0^4 f_0^3} - \frac{\omega_{pe}^2}{\omega_0^2 \epsilon_0} f_0 \beta, \tag{14}$$

$$\frac{d^2 f_s}{dz'^2} = \frac{1}{k_s^2 r_s^4 f_s^3} - \frac{\omega_{pe}^2}{\omega_s^2 \epsilon_0} f_s \beta, \tag{15}$$

where β is given by

$$\beta = \left[\frac{3}{4}\alpha_0 \frac{m_e}{M} \frac{E_{00}^2(z=0)}{r_0^2 f_0^4(z)} e^{-2g_0 z} + \frac{3}{4}\alpha_s \frac{m_e}{M} \frac{E_{s0}^2(z')}{r_s^2 f_s^4(z')} e^{-2g_0 z'}\right]$$
$$\times \exp\left[-\frac{3}{4}\alpha_0 \frac{m_e}{M} \frac{E_{00}^2(z=0)}{f_0^2} e^{-2g_0 z} - \frac{3}{4}\alpha_s \frac{m_e}{M} \frac{E_{s0}^2(z'=0)}{f_0^2} e^{-2g_s z'}\right]. \tag{16}$$

In order to appreciate the effect of self-focusing (hot spot) on SRS backreflectivity, we have derived an expression for the integrated reflectivity (over space only). The integrated reflectivity is the ratio of the scattered power $\int |E_s(z'=0|^2 \, dr_\perp$ to the input power $\int |E_0(z=0|^2 \, dr_\perp$. By using the solution for the scattered field from (13a–c), one obtains the following expression for the integrated reflectivity:

$$R = \frac{E_{s0}^2(z'=0)}{E_{00}^2(z=0)} \left(\frac{r_0^2}{r_s^2}\right) e^{-2g_s(z=0)L_z}. \tag{17}$$

A strategy to minimize SRS is to decrease its spatial gain by decreasing the laser wavelength and increasing the damping Γ_e of the Langmuir waves, which increases with increasing electron temperature or decreasing electron density (Fernandez et al. 1996). Therefore we have obtained numerical results with typical laser fusion parameters: the vacuum wavelength of the laser beam is $\lambda_0 = 351$ nm, the top hot spot f-number is $F = 4$, the electron temperature is taken to be $T_e = 2.5$, 3, 3.5, or 4 keV, and the background density $N_{00} = 0.2\, N_c$, where N_c is the critical density. The intensity of the incident laser beam, I_0 is chosen between 10^{15} and 10^{16} W cm^{-2}, commonly encountered values being $(1\text{–}4) \times 10^{15}$ W cm^{-2}. The seed intensity is 10^{-4} times the maximum intensity of the pump. The results are presented in graphical form in Figs 1–5.

3. Discussion of numerical results

Before proceeding further, we should like to present the dynamical evolution of the pump laser first, namely the creation of the hot spot. To study this, we have numerically solved the system (14) and (15), employing the initial conditions corresponding to a plane wave front of the laser at $z = 0$.

Figure 1 depicts the variation of the dimensionless beam-width parameter f_0 of the pump beam versus the distance of propagation ξ. The solid curve is the case for the undepleted-pump case, while the dashed curve represents the pump-depletion case. It shows that the undepleted beam becomes focused at later ξ. It is obvious from these results that pump depletion affects the self-focusing process of the pump wave significantly. Similarly, Fig. 2 depicts the

https://doi.org/10.1017/S0022377800008898 Published online by Cambridge University Press

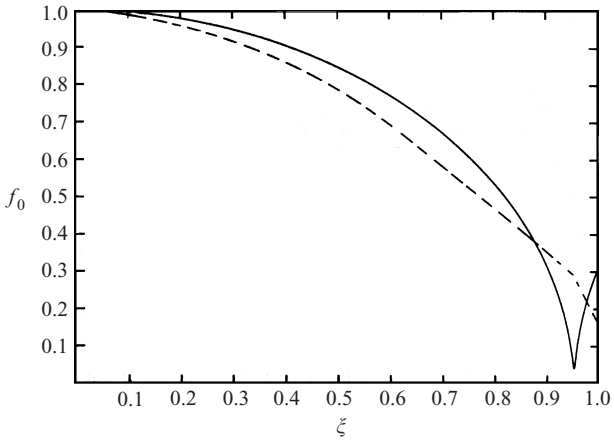

Figure 1. Variation of dimensionless beam-width parameter f_0 of the pump laser beam versus the dimensionless distance of propagation ξ ($= z/R_{d0}$; $R_{d0} = k_0 r_0^2$). The solid line corresponds to the situation without pump depletion, the dashed line corresponds to pump depletion.

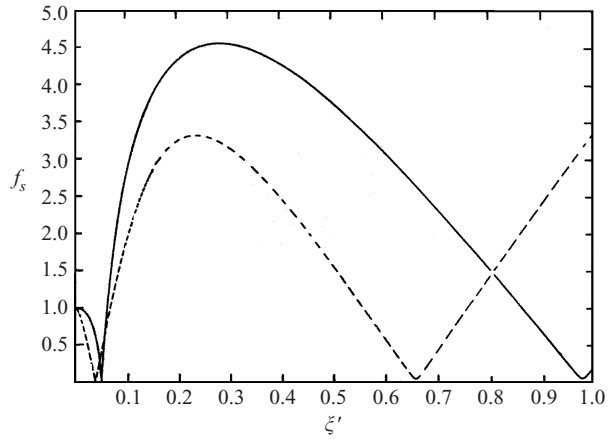

Figure 2. Variation of dimensionless beam-width parameter f_s of the scattered laser beam versus the dimensionless distance of propagation ξ' ($= z'/R_{d0}$). The solid line corresponds to the situation without pump depletion; the dashed line corresponds to pump depletion.

variation of the dimensionless beam-width parameter f_s of the backscattered beam versus the distance of propagation ξ'. It is obvious that the beam first becomes focused and then defocused. The pump-depleted and the undepleted beam exhibit the same behaviour, but their beam widths are different. It is apparent that the effect of pump depletion on the focusing of the scattered wave is significant. This effect of pump depletion on f_0 and f_s can be understood as follows. The dimensionless beam widths of the pump and scattered beam depend on the diffraction (the first term in (14) and (15)) and nonlinear coupling term (the second term in (14) and (15)). For the initially given beam widths of the pump and scattered beams, the diffraction term is not changed much, but the nonlinear coupling term with and without pump depletion changes significantly. Therefore, f_0 and f_s, which depend on the combined effects of diffraction and nonlinear coupling, are affected accordingly.

https://doi.org/10.1017/S0022377800008898 Published online by Cambridge University Press

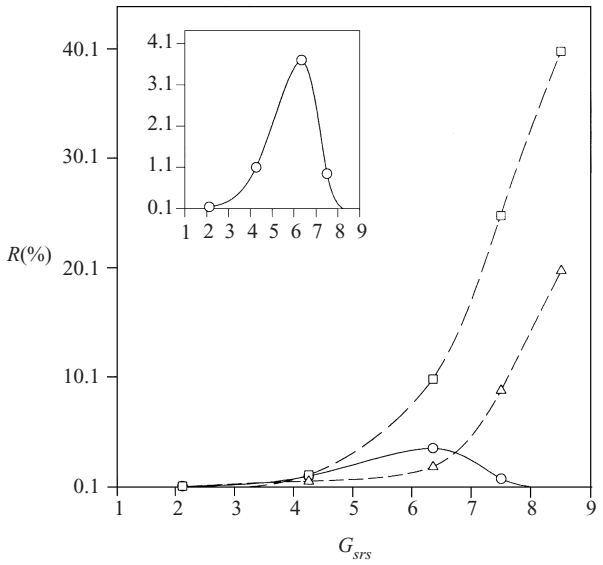

Figure 3. Variation of the integrated reflectivity R versus G_{srs} for $T_e = 2.5$ keV and $N_{00} = 0.2\ N_c$: ○, pump depletion; □, without pump depletion; △, three-wave interaction. The pump-depletion case has also been enlarged in the inset.

In Fig. 3, we summarize the SRS reflectivity calculated from (17) with varying SRS gain G_{srs} at $T_e = 2.5$ keV for the three-wave interaction case and the self-focusing dominated case with and without pump depletion. The results show that the SRS reflectivity increases with G_{srs} for three-wave interaction (triangles) and without pump depletion (squares). The pump-depletion case (circles) has the potential to reduce the SRS reflectivity for gain exponents of more than 6 by a significant factor in this regime. The reason for the maximum reflectivity at an optimum G_{srs} can be explained as follows. The integrated reflectivity depends upon the gain of the scattered beam g_s, (13d). But g_s depends upon the background density as modified by the beam owing to the ponderomotive force and the beam intensity. If, as a result of self-focusing effects, the beam intensity increases and this increased intensity leads to a greater reduction in the background density by the ponderomotive force, then the gain first increases with increasing beam intensity, but later the reduction in density is so large that it decreases the gain. Figure 4 shows the same variation of SRS reflectivity with G_{srs}, but at a higher temperature $T_e =$ 3.5 keV. It is interesting to note here that the SRS reflectivity decreases by a significant factor (of about 3) at higher temperature ($R = 36\,\%$ at $T_e = 2.5$ keV, while $R = 11\,\%$ at $T_e = 3.5$ keV). Our numerical results support the experimental results found by Fernandez et al. (1996) and presented in their Fig. 1. Next, we present numerical results for SRS reflectivity at different $k\lambda_d$ (i.e. different temperatures $T_e = 2.5$, 3, 3.5, and 4 keV) for a peak hot-spot intensity of 3×10^{15} W cm^{-2} and $N_{00} = 0.2\ N_c$. The increases in $k\lambda_d$ lead to an increase in the Landau damping factor Γ_e and a decrease in the SRS reflectivity. These results are presented in Fig. 5.

In order to compare the effects of self-focusing on SRS reflectivity found by ourselves and by Russell et al. (1999), we should like to mention here that, in

https://doi.org/10.1017/S0022377800008898 Published online by Cambridge University Press

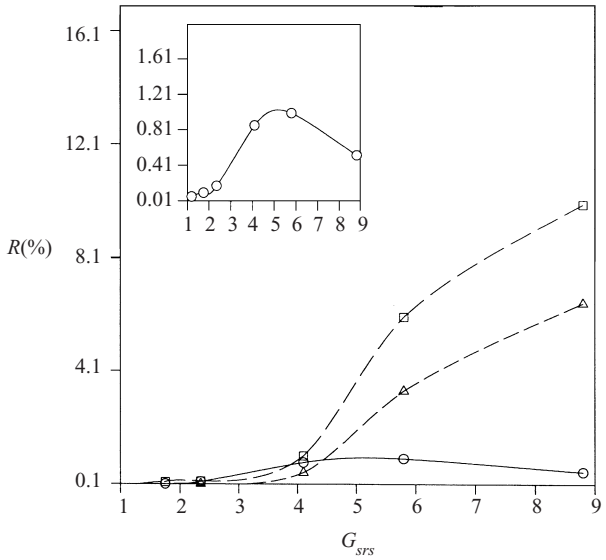

Figure 4. Variation of the integrated reflectivity R versus G_{srs} for $T_e = 3.5$ keV and $N_{00} = 0.2\ N_c$: ○, pump depletion; □, without pump depletion; △, three-wave interaction. The pump-depletion case has also been enlarged in the inset.

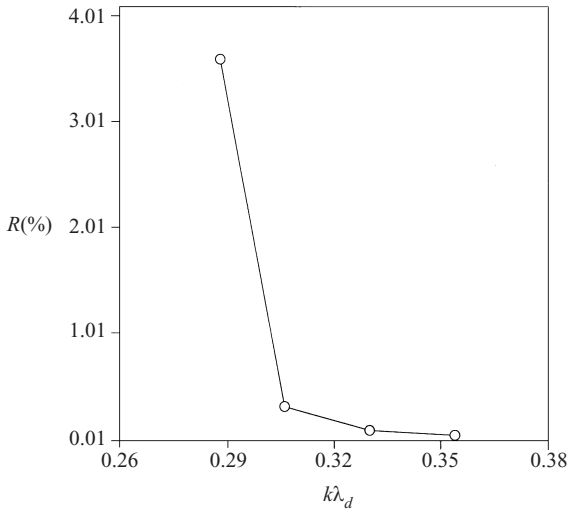

Figure 5. Variation of the integrated reflectivity R versus $k\lambda_d$ for a peak hot-spot intensity of 3×10^{15} W cm^{-2} and $N_{00} = 0.2\ N_c$.

the latter study, they neglected the nA_0 term in the pump-wave equation and the $|A_0|^2$ term in the density equation. This eliminates the density response due to the self-focusing of the laser light and trapping of the light in the ponderomotive channel, and raises the reflectivity by a factor of 3. In our study, we have not neglected these terms; we have studied the SRS reflectivity in the self-focusing case and the three-wave interaction case when no self-focusing is taken into account in the modified density and intensity of the laser beam. Our results show that self-focusing and pump depletion reduce the SRS

https://doi.org/10.1017/S0022377800008898 Published online by Cambridge University Press

reflectivity by a factor of about 3 at the optimum value of G_{srs}. But, in the case of self-focusing without pump depletion, the SRS reflectivity is greater than in the three-wave interaction case and the pump depletion case. Therefore, modified intensity and density modification due to a hot spot play very important roles in affecting the SRS gain and consequently the SRS back-reflectivity.

In summary, we have seen that pump depletion and hot-spot formation affect SRS reflectivity significantly. An optimum value for the reflectivity has also been predicted at about 3×10^{15} W cm^{-2}, and turns out to be $R \approx 4\,\%$ for an electron temperature $T_e = 2.5$ keV.

Acknowledgements

This work was partially supported by the Department of Science and Technology (DST-India) and Indian Council of Cultural Relations (ICCR-India).

References

Akhmanov, S. A., Sukhorakov, A. P. and Khokhlov, R. V. 1968 *Soviet Phys. Usp.* **10**, 609.

Antonsen, T. M. and More, P. 1992 *Phys. Rev. Lett.* **69**, 2204.

Baker, K. L., Drake, R. P., Bauer, B. S., Estabrook, K. G., Rubenchik, A. M., Labaune, C. et al. 1996 *Phys. Rev. Lett.* **77**, 67.

Baker, K. L., Drake, R. P., Estabrook, K. G., Sleaford, B., Prasad, M. K., LaFontaine, B. and Villeneuve, D. M. 1999 *Phys. Plasmas* **6**, 4284.

Berger, R. L., Lefebvre, E., Langdon, A. B., Rothenberg, J. E., Still, C. H. and Williams, E. A. 1999 *Phys. Plasmas* **6**, 1043.

Divol, L. and Mounaix, P. 1998 *Phys. Rev.* **E58**, 2461.

Fernandez, J. C., Cobble, J. A., Failor, B. H., DuBois, D. F., Montgomery, D. S., Rose, H. A. et al. 1996 *Phys. Rev. Lett.* **77**, 2702.

Karttunen, S. J. 1980 *Phys. Rev.* **A23**, 2006.

Kolber, T., Rozmus, W. and Tikhonchuk, V. T. 1993 *Phys. Fluids* **B5**, 138.

Kruer, W. L. 1988 *The Physics of Laser Plasma Interaction*. Addison-Wesley, Redwood City, CA.

Russell, D. A., Du Bois, D. F. and Rose, H. A. 1999 *Phys. Plasmas* **6**, 1294.

Thomson, J. J. 1978 *Phys. Fluids* **21**, 2082.

Tzeng, K. C. and Mori, W. B. 1999 *Phys. Plasmas* **6**, 2105.

Walsh, C. J., Villeneuve, D. M. and Baldis, H. A. 1984 *Phys. Rev. Lett.* **53**, 1445.